Thermochimica Acta, 186 (1991) 187–197
Elsevier Science Publishers B.V., Amsterdam

Characterisation of the thermal genesis course of zinc oxide from zinc acetoacetonate dihydrate

Gamal A.M. Hussien

Chemistry Department, Faculty of Science, Minia University, El-Minia (Egypt)

(Received 10 December 1990)

Abstract

The thermal decomposition course of $Zn(acac)_2$, $Zn(C_5H_7O_2)_2 \cdot 2H_2O$, was characterised to the onset of formation of ZnO. The techniques employed were thermogravimetry (TG), differential thermal analysis (DTA), infrared spectroscopy (IR) and X-ray diffractometry (XRD). The results obtained showed that $Zn(acac)_2$ dehydrates in two consecutive steps at 87 and 110 °C, melts at 143 °C and, then, releases C_3H_4 to yield $Zn(CH_3COO)_2$ at 209 °C. Subsequently, the acetate released CH_3COCH_3 and CO_2 to give $(ZnCO_3)_x \cdot (ZnO)_y$ at 240 °C, which on further heating to 665 °C, decomposed giving ZnO. IR spectroscopy of the gaseous products revealed that a profound chemical reactivity at the gas/solid interfaces was generated throughout the decomposition course. As a result, CH_3COCH_3 was involved in bimolecular interactions over freshly genesised ZnO surfaces, producing CH_4 and $(CH_3)_2C{=}CH_2$ (isobutene) in the gas phase and acetate surface species.

INTRODUCTION

The thermal genesis of metal oxides from inorganic precursors has been widely adopted to obtain technologically important materials [1–5]. Characterisation of the genesis course enables the provision of adequate thermal conditions for producing a solid of specific properties. For instance, metal oxides to be used as refractory materials should fulfil high thermal resistance and mechanical stability requirements [1,5]. Sintering of solid particles should, therefore, be enhanced. In contrast, sintering must be avoided if the oxide is to be used as a catalyst or catalyst support [6]; in catalysis, materials of high surface area are required [7].

Zinc oxide, whose thermal genesis is to be studied in the present investigation, finds numerous applications in various fields. It is an important ingredient in the manufacture of rubber, paint [8], ceramics, glass and cosmetics [8]. It is also employed as a catalyst [9] and as a support for metal catalysts [10] and metal oxide catalysts [10] whose performance has some potential.

The ZnO precursor investigated here is zinc acetoacetonate ($Zn(acac)_2$), $Zn(C_5H_7O_2)_2 \cdot 2H_2O$. The stability constant of this complex is notably high

0040-6031/91/$03.50

[11]. This implies that the acetoacetonate is capable of abstracting Zn ions from media in which its concentration is low. A thorough survey of the literature revealed a single study [12] in which the thermal decomposition of $Zn(acac)_2$ was examined. The results indicated that it decomposes at 130 °C in an inert solvent, such as toluene and xylene, as shown below

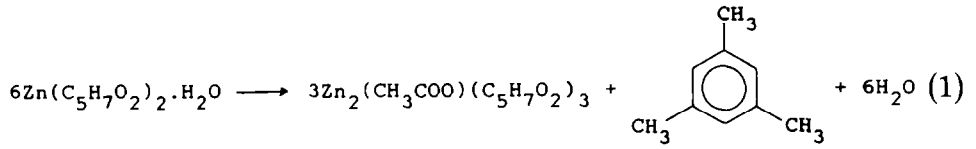

and/or

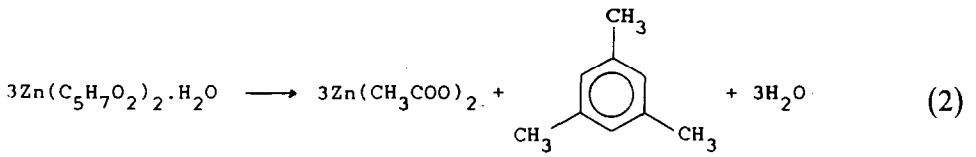

From the above, it is clear that the investigation was not continued to the genesis of ZnO. Therefore, the present investigation examines the decomposition course of $Zn(acac)_2$ dihydrate to the onset of formation of ZnO, using thermogravimetry and differential thermal analysis techniques. The thermal processes encountered were characterised by means of infrared spectroscopy and X-ray diffractometry. In addition, the kinetic parameters (k, A, ΔE) were determined for each process, in the hope of attaining a deeper understanding of the thermal decomposition mechanisms.

EXPERIMENTAL

Zinc acetoacetonate ($Zn(acac)_2$)

The $Zn(acac)_2$, $Zn(C_5H_7O_2)_2 \cdot 2H_2O$, used was 99.8% pure (Aldrich, U.S.A.). From the thermal analyses (see below), the solid-phase decomposition products were obtained by heating at 150–900 °C for 2 h in a dynamic atmosphere of nitrogen (20 ml min^{-1}). The nitrogen gas (99.9% pure, Egyptian Industrial Gases Co., Cairo, Egypt) was dried thoroughly prior to use, by passing it through cold traps (ambient −195 °C) packed with a molecular sieve (4A) and self-indicating silica gel (Merck). The N_2 atmosphere was used to avoid charring the organic moieties.

Thermal analysis

Thermogravimetry (TG) and differential thermal analysis (DTA) of $Zn(acac)_2$ were performed with an automatically recording Shimadzu (Japan)

30-H analyser. Weights of 20 mg were used for the TG, and highly sintered α-Al_2O_3 was the thermally inert reference material for the DTA measurements. TG and DTA curves were recorded on heating up to 1000 °C at various rates ($\theta = 2$, 5, 10 and 20 °C min^{-1}) in a dynamic atmosphere of dry nitrogen (20 ml min^{-1}).

X-ray diffractometry (XRD)

Powder diffractograms of $Zn(acac)_2$ and its solid products of calcination were obtained by means of a model JSX-60 PA Jeol (Japan) diffractometer, equipped with a source of Ni-filtered Cu Kα radiation. For identification purposes, the diffraction patterns ((I/I^0) versus d spacing (Å)) obtained were matched with relevant ASTM standards [13].

Infrared spectroscopy (IR)

Infrared spectra of $Zn(acac)_2$ and its solid products of calcination were obtained at a resolution of 5.3 cm^{-1}, over the frequency range 2000–200 cm^{-1}, using a Perkin–Elmer model 580B double-beam spectrophotometer. The spectra were measured from thin ($\leqslant 20$ mg cm^{-2}), lightly loaded ($< 1\%$ by weight) KBr-supported discs of the test samples.

IR identification of the gaseous decomposition products was from spectra (4000–600 cm^{-1}) of the gas surrounding a 0.5 gm sample of $Zn(acac)_2$, being heated at 10 °C min^{-1} to various temperatures (150–400 °C) for 5 min, in a specially designed IR cell [14]. The cell was equipped with KBr windows, and evacuated to 10^{-2} Torr for 5 min prior to recording the gas phase spectra. The cell background spectrum was ratioed out of the gas phase spectra, using an on-line Perkin–Elmer Data Station (model 3500).

Non-isothermal kinetic analysis of thermoanalytical data

The temperatures (T_{max}) at which the weight-variant (TG) and weight-invariant (DTA) processes are maximised were determined as a function of the heating rate (θ) applied. The kinetic activation energy, ΔE (kJ mol^{-1}), was then calculated for each process from a plot of log θ against $1/T_{max}$, according to the relationship [15]

$$\Delta E = -\frac{R}{b \, \mathrm{dlog}\, \theta/\mathrm{d}(1/T)} \tag{3}$$

where R is the gas constant (8.314 J mol^{-1} °C^{-1}), θ is the heating rate (°C min^{-1}) and b is a constant (0.457).

Calculation of the frequency factor, A (s^{-1}), for the weight-variant processes was carried out, assuming first-order kinetics, using the following

equation [16]

$$\log\left(-\log(1-C)/T^2\right) = \log AR/\theta\Delta E - \Delta E/2.303RT \quad (4)$$

where C is the fraction decomposed at T (T_{max}). The values of ΔE (from eqn. (3)) and A (from eqn. (4)) were used to calculate the rate constant, k (min^{-1}), from the Arrhenius equation

$$k = A\, e^{-\Delta E/RT} \quad (5)$$

RESULTS AND DISCUSSION

The TG and DTA curves recorded for $Zn(acac)_2$ at 20 °C min^{-1} in a dynamic atmosphere of nitrogen are shown in Fig. 1. The curves indicate that $Zn(acac)_2$ decomposes via five endothermic weight-loss processes, namely **I**, **II**, **IV**, **V** and **VI**, maximised respectively at 87, 110, 209, 240 and 665 °C. Process **II** is followed by an endothermic weight-invariant process, **III**, maximised at 143 °C. The T_{max} shifts experienced by the weight-loss processes as a function of the heating rate (θ = 2–20 °C min^{-1}) are indicated in Fig. 2.

Figure 3 shows IR gas-phase spectra, over the frequency range 4000–600 cm^{-1}, from the atmosphere surrounding $Zn(acac)_2$ being heated to various temperatures (150–400 °C) for 5 min. The IR spectra and X-ray powder diffractograms obtained for $Zn(acac)_2$ and its solid decomposition products at 150–900 °C, in an atmosphere of nitrogen, are shown in Figs. 4 and 5, respectively.

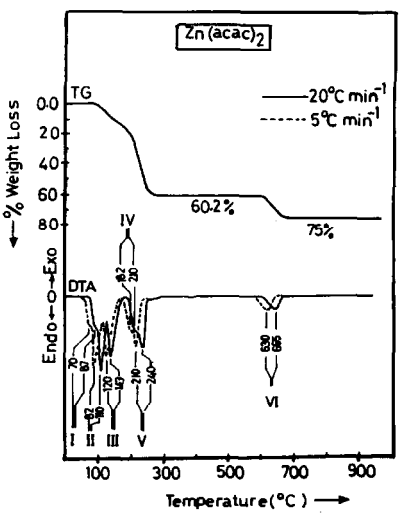

Fig. 1. TG and DTA curves recorded for $Zn(acac)_2$, at the heating rates indicated, in a dynamic (20 ml min^{-1}) atmosphere of nitrogen.

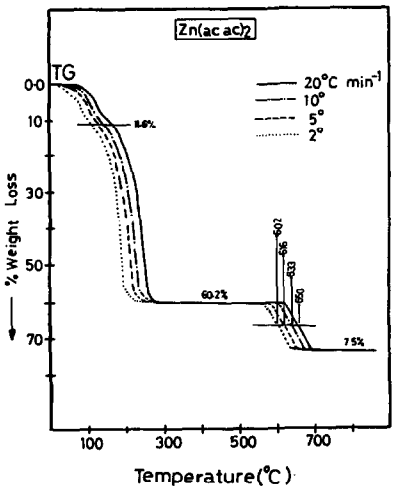

Fig. 2. TG curves recorded for $Zn(acac)_2$ as a function of the heating rates indicated, in a dynamic (20 ml min^{-1}) atmosphere of nitrogen.

The non-isothermal kinetic parameters (k, A, ΔE) determined for the thermal processes encountered throughout the decomposition course of $Zn(acac)_2$ are compiled in Table 1.

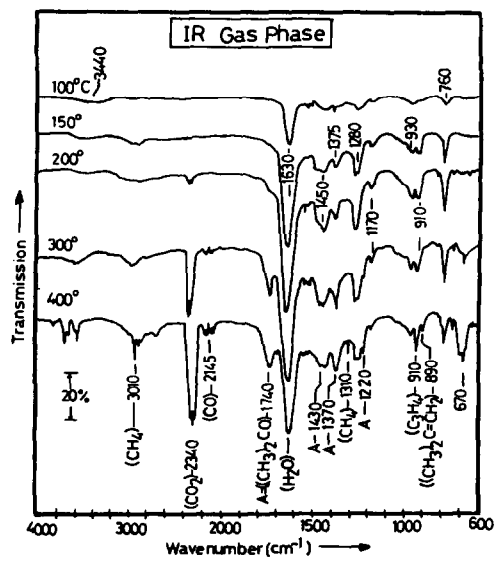

Fig. 3. IR spectra taken at a resolution of 5.3 cm^{-1} from the gas phase surrounding a 0.5 g sample of $Zn(acac)_2$ being heated (at 10 °C min^{-1}) to the temperatures indicated for 5 min.

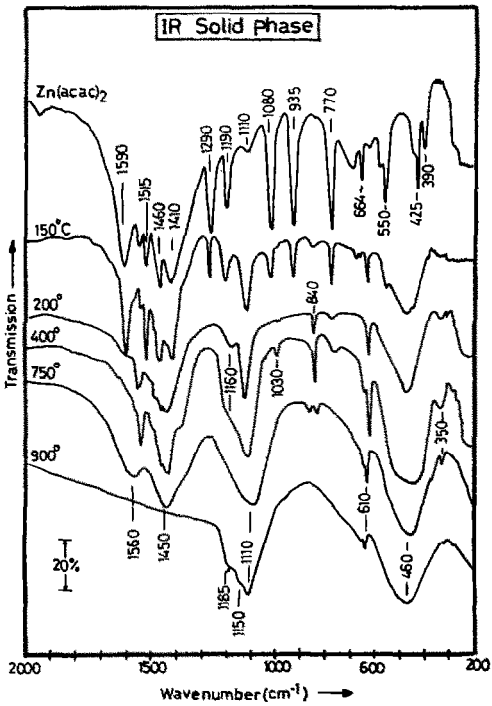

Fig. 4. IR spectra taken at a resolution of 5.3 cm^{-1} from KBr-supported samples of $Zn(acac)_2$ and its solid decomposition products obtained at the temperatures indicated for 2 h, in a dynamic atmosphere of nitrogen.

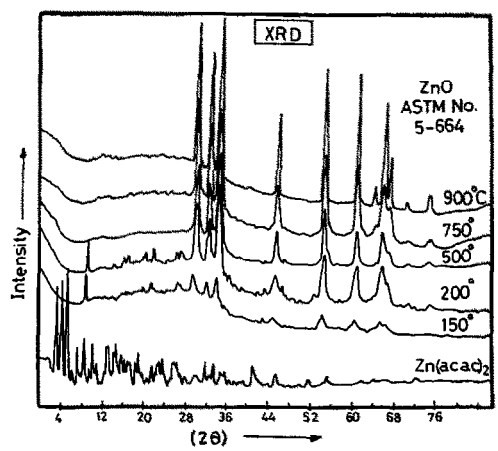

Fig. 5. X-ray powder diffractograms of $Zn(acac)_2$ and its decomposition products obtained at the temperatures indicated for 2 h, in a dynamic atmosphere of nitrogen.

TABLE 1

Non-isothermal kinetic parameters [a] of the processes occurring throughout the decomposition course of $Zn(acac)_2$ in nitrogen atmosphere

Process	k (min^{-1})	log A	ΔE (kJ mol^{-1})
I	3.69×10^{-6}	13.96	56.5
II	3.30×10^{-6}	14.05	61.0
III	–	–	83.5
IV	3.62×10^{-10}	17.56	105.0
V	1.66×10^{-8}	16.28	99.5
VI	3.03×10^{-8}	16.63	181.6

[a] The kinetic parameters for processes **I**, **II**, **IV**, **V** and **VI** were calculated from TG data, whereas for process **III**, DTA data were used.

Processes I and II

From the TG and DTA curves (Fig. 1), it can be seen that processes **I** and **II** are overlapping, endothermic, weight-loss processes, maximised respectively at 87 and 110 °C. The total weight loss effected (11.6%) through both processes is fairly close to that expected (12.01%) for the release of two moles of water, i.e.

$$Zn(C_5H_7O_2)_2 \cdot 2H_2O \xrightarrow{I} Zn(C_5H_7O_2)_2 \cdot H_2O \xrightarrow{II} Zn(C_5H_7O_2)_2 \quad (6)$$

The corresponding activation energies (Table 1) have values (56.5 (**I**) and 61 (**II**) kJ mol^{-1}) within the range characteristic of dehydration processes ($\geq$ 60 kJ mol^{-1}) [17].

In support of the above results, the IR gas-phase spectrum at 100 °C (Fig. 3) has a broad, weak absorption centred around 3440 cm^{-1} and a strong absorption at 1630 cm^{-1}, due to the ν (OH) and δ (HOH) vibrations, respectively, of water molecules [11]. These absorptions intensify further in the 150 °C spectrum. The weak absorptions between 1550 and 700 cm^{-1} are most probably associated with a possible increase in the vapour pressure of the material. The IR spectrum of the solid-phase decomposition product at 150 °C (Fig. 4) bears a great deal of similarity to that obtained for untreated $Zn(acac)_2$. It displays bands at 1590, 1515, 1460, 1410, 1290, 953 and 770 cm^{-1}, which are assignable to the vibration modes of the acetoacetonate complex [11]. The spectrum also displays bands at 664, 550 and 410 cm^{-1} due to ZnO stretching vibrations [11]. However, the XRD of the solid product at 150 °C (Fig. 5), when compared to that of $Zn(acac)_2$, indicates an effective loss of crystal coherency. In fact, it reveals a predominantly amorphous nature.

Process III

Process **III** (Fig. 1) is an endothermic, weight-invariant process maximised at 143° C. It takes place immediately following the completion of process **II**. A preliminary examination indicated that $Zn(acac)_2$ melts near 140° C so that process **III** can be attributed to melting, which explains the amorphous character of the solid yielded at 150° C (Fig. 5) as seen in the XRD results. The activation energy (85.5 kJ mol^{-1}) determined for process **III** is of the same order of magnitude as solid state fusion energies [17].

Process IV

The TG curve (Fig. 1) shows that process **IV** takes place endothermically (DTA) at $T_{max} = 209$° C, largely overlapping with the succeeding process, process **V**. The IR gas-phase spectra at 150 and 200° C (Fig. 3) exhibit, in addition to water absorptions, absorption bands assignable to C_3H_4 [18], i.e. CH_3–C≡CH, at 1450, 930, 910 and 760 cm^{-1}. The release of C_3H_4 accounts for the decomposition of $Zn(acac)_2$ to zinc acetate, according to

$$Zn(C_5H_7O_2)_2 \rightarrow Zn(CH_3COO)_2 + 2C_3H_4 \quad (7)$$

The IR spectrum of the decomposition solid product at 200° C (Fig. 4) displays characteristic bands due to acetate (at 1560, 1430 and 1160 and 1030 cm^{-1}) [11]. The difference ($\Delta\nu = 130$ cm^{-1}) between ν_{as} (1560 cm^{-1}) and ν_s (1430 cm^{-1}) of the COO^- vibrations suggests that the acetate groups are bridge-bonded to the Zn ions [19]. The kinetic energy calculated for process **IV** amounts to 105 kJ mol^{-1}.

Process V

Process **V** (Fig. 1) is endothermic, largely overlapping with process **IV**; it maximises at 240° C. The total weight loss determined on completion of process **V** is 60.2%, which is near to that expected (58.01%) for the formation of $ZnCO_3$ from $Zn(C_5H_7O_2)_2 \cdot 2H_2O$. Thus, the reaction involves the decomposition of zinc acetate to zinc carbonate, as follows

$$Zn(CH_3COO)_2 \rightarrow ZnCO_3 + CH_3COCH_3 \quad (8)$$

Reaction (8) is corroborated by the IR spectra taken from the gas phase at 200 and 300° C (Fig. 3), in which absorptions characteristic of acetone (at 1740, 1430, 1370 and 1220 cm^{-1}) [18] are observed. The gas phase spectra display, moreover, absorptions due to CO_2 (at 2340 and 670 cm^{-1}) [18] and CO (at 2145 cm^{-1}) [18], which could be considered consistent with the decomposition of $ZnCO_3$ to ZnO. It is worth mentioning that $ZnCO_3$ decomposes reportedly [20] at 300° C to given ZnO.

The solid product at 300 °C gave an IR spectrum (Fig. 4) which shows the disappearance of the acetate absorption bands and the appearance of absorptions assignable to carbonate species (at 1560, 1450, 840 and 610 cm^{-1}) [12].

It is worth noting, however, that the XRD analysis of the solid products yielded at 200–400 °C detected only crystalline ZnO. This implies that the product of process **V** is not $ZnCO_3$ alone, but most likely a multi-component material, probably including carbonate and oxide species of zinc that are somehow isostructural, e.g. $(ZnCO_3)_x \cdot (ZnO)_y$. Therefore, it is practically impossible, in the light of these results, to derive any firm conclusions from the thermogravimetric analysis as to the exact composition of the solid product at 300 °C. Nevertheless, thermogravimetry can confirm that the product of process **V** is thermally stable over a wide range of temperatures (300–650 °C). The energy of activation determined for process **V** (99.5 kJ mol^{-1}) is close to that determined (105 kJ mol^{-1}) for process **IV**, thus explaining the overlap of these two processes (Fig. 1).

Process VI

The TG curve (Fig. 1) shows that thermal process **VI** occurs in the temperature range between 618 and 655 °C, with a weight loss of 14.8%, which brings the total weight loss to 75%, very close to that expected (72.69%) for the decomposition of $Zn(C_5H_7O_2)_2 \cdot 2H_2O$ to ZnO. Thus, process **VI** involves primarily the decomposition of the mixed Zn carbonate and oxide to ZnO.

The IR spectrum of the calcination product at 300 °C (Fig. 4) displays absorption bands due mainly to carbonate species, whereas the 750 °C spectrum exhibits bands due to ZnO (at 350, 460 and 610 cm^{-1}) [21]. At 900 °C, the spectrum (Fig. 4) shows that the bands due to the carbonate species have completely disappeared: it detects only pure ZnO. The bands observed at 1185, 1150 and 1110 cm^{-1} are most probably due to charged molecular oxygen species [22], which are frequently encountered on non-stoichiometric metal oxide surfaces. It was reported earlier [23], that ZnO contains interstitial Zn atoms, which recombine with oxygen, at least on the surface, to produce O_2^{x-} species.

The XRD of the calcination products formed between 500 and 900 °C exhibit (Fig. 5) a pattern identical to that of ZnO (ASTM No. 5-664). The crystallinity is shown to improve markedly with temperature.

The energy of activation of process **VI** amounts to 181.6 kJ mol^{-1}, higher than that reported (96 kJ mol^{-1}) [6] for $ZnCO_3$ decomposition, thus providing additional evidence for the complexity of the solid material involved in process **VI** ($(ZnCO_3)_x \cdot (ZnO)_y$).

Chemical reactivity at the gas–solid interface

The IR spectrum of the gas phase at 400 °C displays absorption bands characteristic of methane and isobutene; their locations are indicated in Fig. 3 and assignments are given in ref. 24. These gases are not amongst the initial decomposition products of $Zn(acac)_2$. Moreover, the 400 °C gas-phase spectrum indicates a slight decrease in the absorptions characteristic of acetone molecules.

It has been established [24] that the formation of methane and isobutene in the presence of metal oxide catalysts is due to the involvement of acetone molecules in a surface-mediated bimolecular reaction, through which acetone is adsorbed and, hence, activated for an aldol-condensation-like process

$$(CH_3)_2CO(s) + OH^-(s) + (CH_3)_2CO(g) \rightarrow (CH_3)_2C{=}CH_2(s) + CH_3COO^-(s) \quad (9)$$

where (s) indicates surface. Simultaneously, the adsorbed acetone is also exposed to a nucleophilic attack by an adjacent surface OH^-, with loss of a methyl group in the form of CH_4 [2,24–26]

$$(CH_3)_2CO(s) + OH^-(s) \rightarrow CH_4(g) + CH_3COO^-(s) \quad (10)$$

It should be noted that both reactions (9) and (10) produce acetate surface species. This may explain the indications of acetate surface species in the IR spectra up to 750 °C (Fig. 5).

CONCLUSIONS

The following conclusions can be drawn from the above presented and discussed results:

1. The course of the thermal genesis of ZnO from zinc acetoacetonate dihydrate may include the following pathways

$$Zn(C_5H_7O_2)_2 \cdot 2H_2O \xrightarrow{I} Zn(C_5H_7O_2)_2 \cdot H_2O \xrightarrow{II} Zn(C_5H_7O_2)_2 \xrightarrow{III}$$

$$Zn(C_5H_7O_2)_2(melt) \xrightarrow{IV} Zn(CH_3COO)_2 \xrightarrow{V} (ZnCO_3)_x \cdot (ZnO)_y \text{ mixed phase} \xrightarrow{VI} ZnO$$

where the Roman numerals denote the accompanying thermal processes (see Table 1).

2. The evolution of acetone rather than acetic acid through the decomposition of the intermediate zinc acetate is a typical behaviour of acetates of irreducible metal ions [27].

3. The conversion of acetone to methane and isobutene indicates that the observed gaseous decomposition products are not always formed directly in the initial stages, and may be due to reactions between intermediate products.

4. Reactions occurring at the gas–solid interface throughout the decomposition course may provide some useful conclusions regarding the catalytic behaviour of the associated solid products.

ACKNOWLEDGEMENT

The author thanks Prof. M.I. Zaki of Minia University for his critical reading of the manuscript and his enlightening discussions.

REFERENCES

1 S.A.A. Mansour, G.A.M. Hussien and M.I. Zaki, Thermochim. Acta, 150 (1989) 153.
2 S.A.A. Mansour, G.A.M. Hussien and M.I. Zaki, Reactivity of Solids, 8 (1990) 197.
3 S.A.A. Mansour, M.A. Mohamed and M.I. Zaki, Thermochim. Acta, 129 (1988) 189.
4 J.D. Danforth and J. Dix, J. Am. Chem. Soc., 93 (1971) 6843.
5 M. Le Van, G. Perinet and P. Bianco, Bull. Soc. Chim. Fr., (1968) 3104.
6 B. Delmon, P. Grange, P.A. Jacobs and G. Poncelet (Eds.), Preparation of Catalysts, Vol. II, Elsevier, Amsterdam, 1979.
7 G.A.M. Hussien, N. Sheppard, M.I. Zaki and R.R. Fahim, J. Chem. Soc. Faraday Trans. I, 85(7) (1989) 1732.
8 C.H. Bates, W.B. White and R. Roy, Science, 137 (1962) 993.
9 G.D. Mariadassou and L. Davignon, J. Chem. Soc. Faraday Trans. I, 78 (1982) 2447.
10 A. Zecchina, S. Coluccia and C. Morterra, Appl. Spectrosc. Rev., 21(3) (1985) 259.
11 K. Nakamoto, Infrared Spectra of Inorganic and Coordination Compounds, John Wiley and Sons, New York, 1970, p. 253.
12 G. Rudolph and M.C. Henry, Inorg. Chem., 3 (1964) 1317.
13 J.V. Smith (Ed.), X-ray Powder Data File, American Society for Testing Materials, Philadelphia, 1960.
14 J.B. Peri and R.H. Hannan, J. Phys. Chem., 64 (1960) 1526.
15 J.H. Flynn, J. Therm. Anal., 27 (1983) 45.
16 A.W. Coats and J.P. Redfern, Nature, 201 (1964) 68.
17 W.E. Brown, D. Dollimore and A.K. Galway, in C.H. Bamford and C.E.H. Tipper (Eds.), Chemical Kinetics, Vol. 22, Reactions in the Solid State, Elsevier, Amsterdam, 1980, p. 130.
18 R.H. Pierson, A.M. Fletcher and E.St. Clair Gabtz, Anal. Chem., 28 (1956) 1218.
19 D.M. Griffiths and C.H. Rochester, J. Chem. Soc. Faraday Trans. I, 74 (1987) 403.
20 H.-P. Boehm, Discuss. Faraday Soc., 25 (1971) 264.
21 J.A. Gadsden, Infrared Spectra of Minerals and Related Compounds, Butterworths, London, 1975, p. 103.
22 F. Al-Mashta, N. Sheppard, V. Lorenzelli and G. Busca, J. Chem. Soc. Faraday Trans. I, 78 (1982) 979.
23 B.M. Arghiropoulos and S.J. Teichner, J. Catal., 3 (1964) 477.
24 M.I. Zaki and N. Sheppard, J. Catal., 80 (1983) 114.
25 A.V. Kiselev and A.V. Uvarov, Surf. Sci., 6 (1967) 399.
26 A.V. Deo, P.T. Chuang and I.G. Dalla Lana, J. Phys. Chem., 75 (1971) 234.
27 M.D. Judd, B.A. Plunkett and M.I. Pope, J. Therm. Anal., 6 (1974) 555.